Coordination Chemistry Reviews 257 (2013) 3323–3331

Contents lists available at ScienceDirect

Coordination Chemistry Reviews

journal homepage: www.elsevier.com/locate/ccr

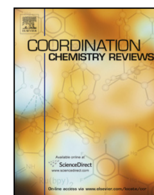

Review

Mechanisms and reactions during atomic layer deposition on polymers

Gregory N. Parsons [a,*], Sarah E. Atanasov [a], Erinn C. Dandley [a], Christina K. Devine [a], Bo Gong [a], Jesse S. Jur [b], Kyoungmi Lee [a], Christopher J. Oldham [a], Qing Peng [a], Joseph C. Spagnola [a], Philip S. Williams [a]

[a] Department of Chemical and Biomolecular Engineering, North Carolina State University, Raleigh, NC 27695, United States
[b] Department of Textile Engineering, Chemistry and Science, North Carolina State University, Raleigh, NC 27695, United States

Contents

1. Introduction 3323
2. Surface versus sub-surface ALD 3324
3. Mechanisms of ALD on polymers 3324
   3.1. Polyolefin (polypropylene) 3325
   3.2. Polyvinyl alcohol 3326
   3.3. Polyamide-6 3327
   3.4. Poly(methyl methacrylate) 3328
   3.5. Polyesters 3328
   3.6. Quantitative analysis 3329
4. Discussion 3329
5. Summary 3330
   Acknowledgement 3330
   References 3330

ARTICLE INFO

Article history:
Received 10 April 2013
Accepted 2 July 2013
Available online 24 July 2013

Keywords:
Atomic layer deposition
Polymers
Thin films
Inorganic coatings
Al_2O_3

ABSTRACT

There is significant growing interest in atomic layer deposition onto polymers for barrier coatings, nanoscale templates, surface modification layers and other applications. The ability to control the reaction between ALD precursors and polymers opens new opportunities in ALD materials processing. It is well recognized that ALD on many polymers involves subsurface precursor diffusion and reaction which are not encountered during ALD on solid surfaces. This article reviews recent insights into chemical reactions that proceed during ALD on polymers, with particular focus on the common Al_2O_3 reaction sequence using trimethyl aluminum (TMA) and water. We highlight the role of different polymer reactive groups in film growth, and how the balance between precursor diffusion and reaction can change as deposition proceeds. As a strong Lewis acid, TMA forms adducts with Lewis base sites within the polymer, and the reactions that proceed are determined by the neighboring bond structure. Moreover, the Lewis base sites can be saturated by TMA, producing a self-limiting half-reaction within a three-dimensional polymer, analogous to a self-limiting half-reaction commonly observed during ALD on a solid planar surface.
© 2013 Elsevier B.V. All rights reserved.

1. Introduction

Polymers are important as barrier materials, protective coatings, resist materials in semiconductor logic and memory device fabrication, and polymer fibers are widely found in gas and liquid filters, as well as in textiles and a growing range of nonwoven materials applications. Surfaces of these materials are often modified, for example, to improve barrier properties, control surface adhesion, achieve biofunctionality, and modify surface wetting [1–5]. Plasma and physical vapor deposition methods are often used, but vapor-phase atomic layer deposition (ALD) can offer some significant advantages over other techniques. Many thermal ALD processes for metal oxides and metals proceed readily at temperatures compatible with polymer substrates, even as low as room

* Corresponding author. Tel.: +1 919 515 7553.
E-mail address: parsons@ncsu.edu (G.N. Parsons).

0010-8545/$ – see front matter © 2013 Elsevier B.V. All rights reserved.
http://dx.doi.org/10.1016/j.ccr.2013.07.001

temperature [6]. The exothermic reaction can promote covalent bonding with the substrate to improve adhesion, for example. The self-limiting binary reaction sequence that is well known in ALD allows the surface coating or modification process to be conformal and uniform across a large surface area substrate. However, when polymer substrates are used, even under conditions where the ALD precursor and reactant are known to undergo a controlled self-limited reaction on a solid surface, the precursor interaction with the polymer substrate may not be self-limiting. This will lead to a polymer/inorganic interface that depends strongly on the polymer and the metal precursor as well as other detailed deposition conditions.

A recent review discussed previous studies of ALD on organic materials, including small molecules, polymers and self-assembled monolayers [7]. Applications for ALD on soft materials are very broad [8], and ALD has been studied on many different synthetic and natural polymer systems including polyimide [9–11], polyethylene terephthalate [12], polyethylene [13], polystyrene [14,15], polypropylene [14,16–18], polyamide-6 [16,19,20], polymethyl methacrylate [14,21–24], polylactic acid [18], polyvinyl chloride [14], polyvinyl alcohol [24,25], polyethylene naphthalate [11,24], poly(ether ether ketone) [21], poly(tetrafluoro ethylene) [21], polydimethylsiloxane [26,27], ethylene tetrafluoroethylene [21], polyethylene imine [28], polyethersulfone [29], cellulose cotton [5,30–34], spider silk [35] and others. As the number of studies expands, there is a need to improve understanding of the interactions between the ALD precursor and the polymer's physical and chemical structure.

Studies of ALD processes on natural polymers show that precursors can infiltrate and react to alter, and sometimes significantly improve the material's mechanical properties [35]. The extent of reaction between the polymer and the vapor precursor can be increased by extending the exposure time per cycle in the ALD sequence, and/or by performing multiple short pulses of the precursor reactant without including a co-reactant step. The technique can be termed Multiple Pulse Vapor Infiltration (MPI), Sequential Vapor Infiltration (SVI), or other names [6,8]. Exposure to water vapor, either in the reactor or in the air after removal from the reactor, allows the reaction to go to completion, producing a hybrid organic/metal oxide network polymer [36].

Polymers often perform well as sacrificial nanostructured template to form oxide spheres, nanotubes or other shapes [37,38]. When the ALD coating produces a good conformal film, dissolving the polymer leaves an inorganic shell mimicking the outer surface of the 3D template. When the precursor substantially diffuses into the polymer, a calcination step after reactant exposure can lead to a solid 3D structure [36]. However, if the connectivity between the inorganic sites within the solid is poor, calcination produces a shapeless powder. ALD-infiltration of patterned polymers on a surface followed by calcination or oxidation can produce patterned oxide lines that may then be used, for example, as a nanoscale etch resist [39].

For all of these material systems, a good understanding of the fundamental interactions between organic functional groups and inorganic precursors will be important to achieve and utilize new applications. Most published work for ALD on polymers addresses Al_2O_3 ALD from trimethyl aluminum (TMA) and water. Xu and Musgrave [40] undertook a density functional theory study of Al_2O_3 ALD on organic monolayers with various end terminations. Reactions between TMA and a functional group in the polymer generally proceed by first forming a Lewis acid/base adduct intermediate. As a strong Lewis acid, TMA will form an adduct with the most Lewis basic sites in the polymer, typically an oxygen lone-pair. A transition through a kinetic barrier leads to the final product state. Often, the transition state barrier is relatively small (i.e. less than 25–30 kcal/mol), so the reaction will proceed at low temperature. These reaction schemes were calculated for reaction between one functional group and one TMA molecule. In addition, TMA is also a strong Lewis acid catalyst [41], so TMA bound in an adduct state may enhance reactivity for a second TMA with the organic.

Generally, the reactions that occur during ALD on these materials will depend on the nature of the polymer and the chemistry of the precursor and co-reactant used during ALD. This article discusses recent studies of reaction mechanisms during TMA/water or other ALD processes on several different polymer materials. The results suggest guidelines that may be helpful to understand ALD reactions on a range of other organic materials. Improved knowledge will help enable new ALD processes to achieve better inorganic/organic film integration for future applications and materials systems.

2. Surface versus sub-surface ALD

Atomic layer deposition on hard surfaces proceeds through reactive sites available on the growth surface. However, for polymers, reactive sites may or may not be present, and many polymers are permeable to small molecules, allowing ALD precursors to move in and out of the near surface and bulk of the polymer substrate. Some polymers therefore allow ALD that mimics that on solid surfaces, while others result in very different final reaction products.

A schematic diagram for an ideal TMA/water ALD processes on a polymer surface (in this case, a polymer fiber) that contains a large density of reactive surface groups that can react with TMA is shown in Fig. 1. Cellulosic cotton is an example of a natural polymer with a large density of surface hydroxyl groups, and Fig. 1 shows a transmission electron microscopy (TEM) image of a cotton fiber after many TMA/water cycles. The organic/inorganic interface is fairly abrupt (within the resolution of the image).

An abrupt, well-defined polymer/inorganic interface is not commonly observed after ALD on most polymers. Fig. 2 shows a similar schematic diagram for TMA/water on a polypropylene, a polyolefin that lacks reactive groups for ALD nucleation. In this case, the precursor does not readily react on the surface, but instead diffuses sub-surface, leading to polymer swelling, subsurface particle growth and rough surface texture. A TEM image of a polypropylene fiber coated using TMA/water at 90 °C shows the nonuniform film structure and rough surface texture that results after ALD [17].

Several studies of ALD on organic monolayers also show that the surface termination of the polymer, as well as the precursor size and ligand structure all contribute to the final product [28,42–44]. Useful polymers can contain many, some or very few reactive functional groups on their polymer chain. While reactive functional groups will provide sites for film nucleation and growth, polymers with functional groups available on the surface do not always result in smooth conformal film growth as expected for ALD on a solid inorganic substrate.

3. Mechanisms of ALD on polymers

This section reviews mechanisms of Al_2O_3 ALD on polyolefin (polypropylene, PP), polyvinyl alcohol (PVA), polyamide-6 (PA-6), poly(methyl) methacrylate (PMMA), as well as poly(ethylene terephthalate) (PET), and poly(butylene terephthalate) (PBT), as example polyesters. These materials are common polymers that present different bonding structures for ALD film nucleation and growth. Polyolefins consist of alkyl chains which are typically considered non-reactive groups. The PVA and PMMA contain functional units (hydroxyls and/or carbonyls) in pendant groups off the polymer chain. The polyamide and polyesters contain amine and/or carbonyl groups within the polymer backbone. The specific interaction mechanism for trimethyl aluminum reaction with the carbonyl

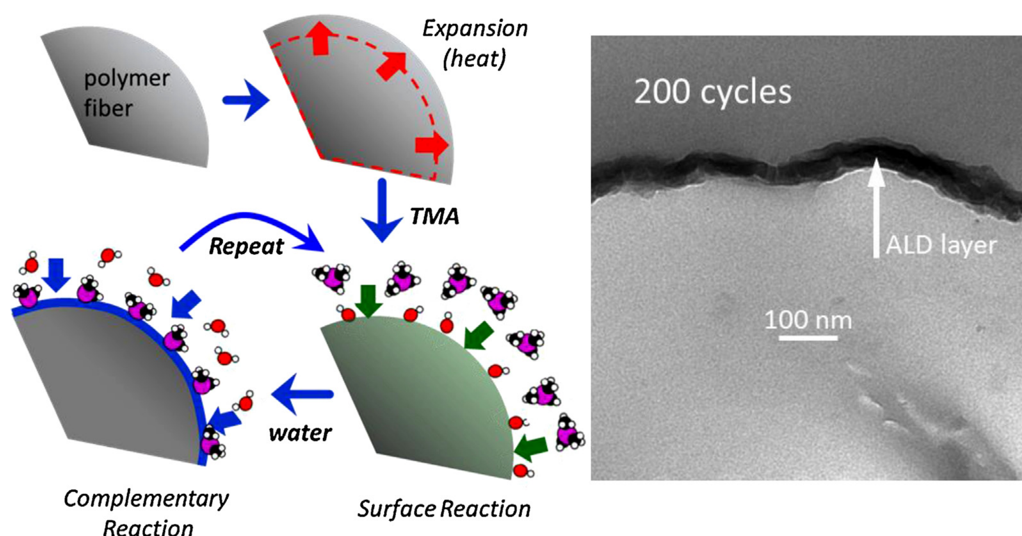

Fig. 1. Schematic reaction scheme for atomic layer deposition of aluminum oxide on a polymer displaying hydroxyl functional groups. The ALD cycle repeats to form a well-defined overcoat on the polymer. The image is of 200 cycles of Al_2O_3 ALD coating on cellulose cotton polymer, showing a relatively abrupt polymer/oxide interface.
Adapted from Ref. [7].

group depends on the location and environment of the carbonyl within the polymer.

3.1. Polyolefin (polypropylene)

Polypropylene is a common chemically inert, semicrystalline, nonpolar thermoplastic polymer with a glass transition temperature, T_g, near −10 °C, and the melting point is ∼165–176 °C. The polymer softening point is ∼90 °C, but it can withstand coating processes for short times (minutes to hours) at 120 °C. The coefficient of linear expansion for polypropylene is $\sim(0.6–1.1)\times10^{-4}\,°C^{-1}$ between 60 and 90 °C which is larger than most common polymers. Its surface is hydrophobic, and it is resistant to organic and inorganic acids, alcohols, esters, ketones, and alkalis. Wilson et al. [14] studied ALD of the TMA/water process on polypropylene using a quartz crystal microbalance (QCM) and concluded that TMA diffused into the polymer bulk leading to sub-surface reaction during the water exposure step. In

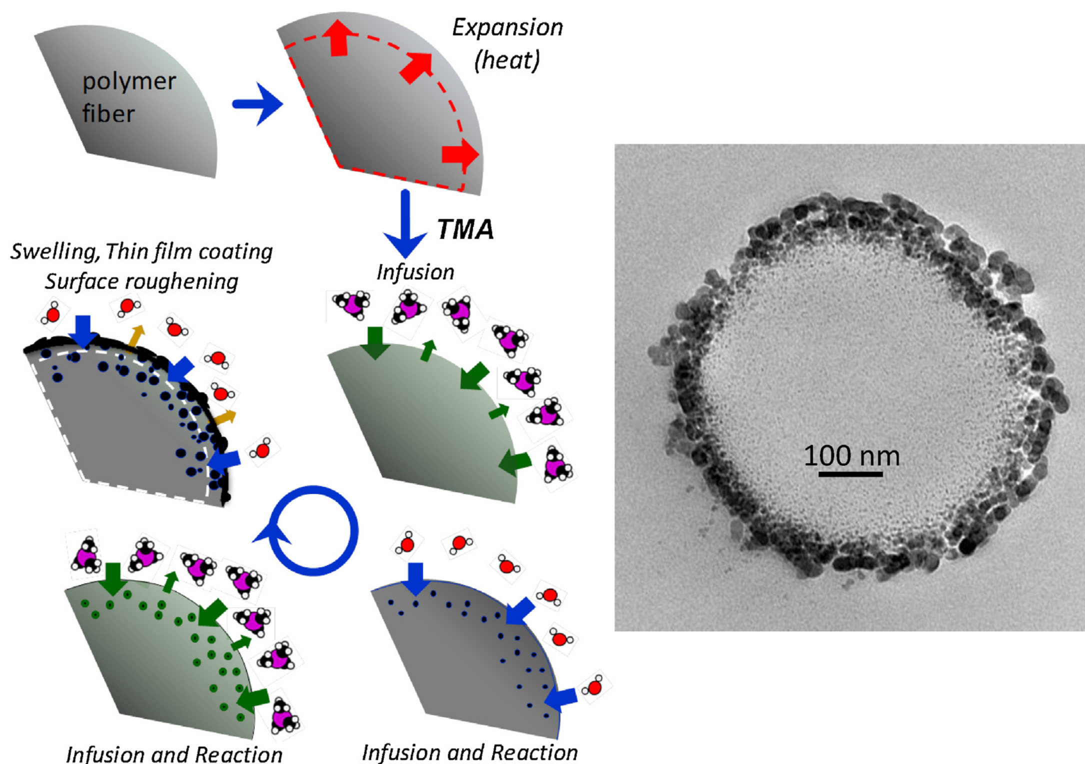

Fig. 2. Schematic for Al_2O_3 ALD on a polymer without functional groups. The metal organic (TMA) and/or reactant (water) can be absorbed into the polymer. Repeated ALD cycles result growth in sub-surface particles along with swelling and roughening of the substrate. A TEM image shows a polypropylene fiber after coating using TMA/water at 90 °C, producing a graded polymer/inorganic interface and rough surface texture.
Adapted from Ref. [7].

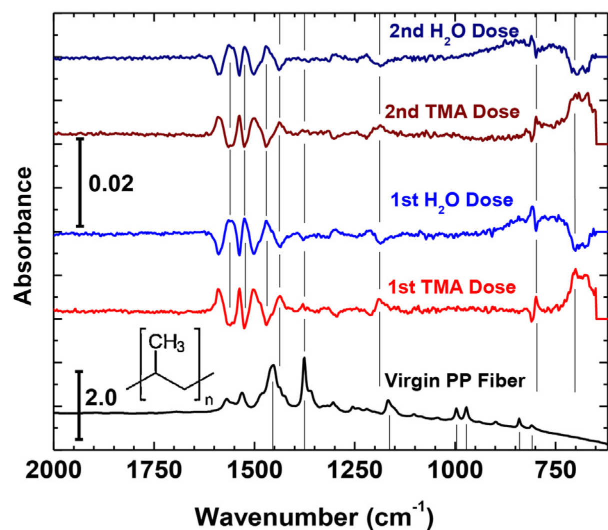

Fig. 3. Differential infrared transmission data collected during TMA/water ALD at 90 °C on polypropylene. The data shows changes consistent with diffusion of precursor reactants into the polymer without substantial reaction.
Adapted from Ref. [26].

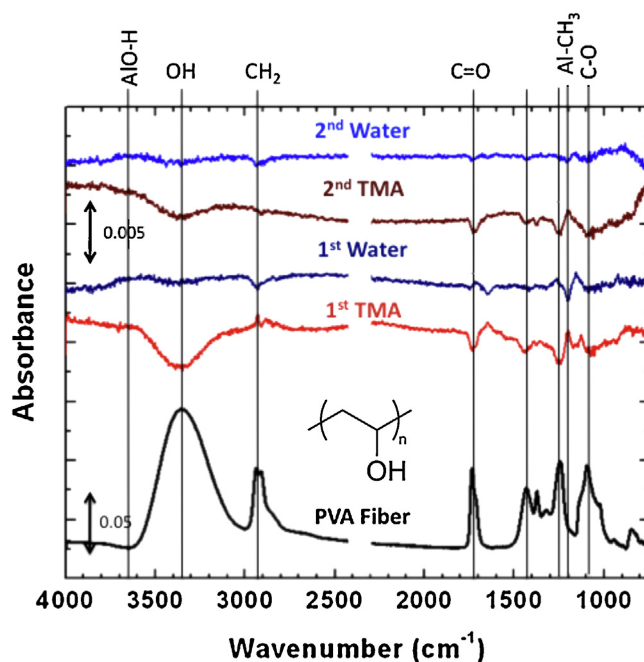

Fig. 4. Infrared transmission data during TMA/water exposures onto PVA nanofibers at 90 °C. TMA exposure consumes OH groups and produces Al—CH_3 groups as expected for ALD on the surface of the polymer.
Adapted from Ref. [26].

subsequent studies, Spagnola et al. [16], Jur et al. [17], and Gong and Parsons [24] studied ALD Al_2O_3 onto polypropylene using QCM, FTIR and transmission electron microscopy. They found that substrate temperature had a strong influence on the extent of subsurface diffusion and the surface roughness of the deposited film. At lower deposition temperatures (~60 °C) the precursors diffused less into the polymer bulk, resulting in a relatively smooth polymer/inorganic interface. For deposition at 90 °C, substantial subsurface diffusion occurred, creating a graded interface and a rough top surface.

Results from FTIR studies of the reactions between polypropylene and the TMA/H_2O ALD reactants at 90 °C are shown in Fig. 3 [16]. The substrate for these studies was a polymer fiber mat with a relatively large surface area located in the deposition zone of an ALD reactor. Polymers studied were held under vacuum overnight to remove any adsorbed water. The IR transmission was collected from the starting substrate at the deposition temperature, and differential spectra were collected during the inert gas purge after each half-cycle using the most recent collected spectrum as the background. The difference spectra are multiplied by 100× compared to the background. Polypropylene shows modes [45] associated with —CH_2 scissors at 1452 cm^{-1}, —CH_3 deformation at 1375 cm^{-1}, C—C stretching + —CH_3 rocking + C—H bend at 1166 cm^{-1}, and —CH_3 rocking + CH bending at 997 cm^{-1}, —CH_3 rocking + C—C stretching at 971 cm^{-1}, and CH_2 rocking near 841 and 810 cm^{-1}. Modes near 1550 and 1640 cm^{-1} are ascribed to some oxidation of the polypropylene backbone resulting in blue shift of the C—H scissors deformation and combination modes. This is also consistent with weak features near 1200 cm^{-1} associated with C—O stretching. After TMA exposure, peaks appear at 1437 cm^{-1}, 1190 cm^{-1}, and 706 cm^{-1} due to CH_3 rocking, and CH_3 symmetric and asymmetric deformation, respectively [45], indicating TMA on or within the polymer. TMA exposure also leads to changes in the CH_2 bending modes resulting in an oscillatory shape in the difference spectra between 1450 and 1600 cm^{-1}. A shift in the CH_2 bending modes can be ascribed to changes in C—H bond polarization or due to deformation of the crystallite regions when TMA penetrates into the polymer network [16]. The water exposure step produces the opposite change in C—H modes between 1450 and 1600 cm^{-1} consistent with some out-diffusion of TMA. Some TMA will remain in the polymer and react with water during the reactant pulse, producing sub-surface film nucleation and subsequent growth during following ALD steps. The Al—CH_3 features also decrease consistent with Al—OH formation. The net change in the IR spectrum after the TMA/H_2O cycle indicates little change in chemical structure of the polypropylene. A cross-sectional TEM image of polypropylene fibers after 100 cycles of TMA/water exposure at 90 °C is shown in Fig. 2 showing significant sub-surface nucleation. A large mass uptake is also observed at 90 °C using in situ QCM analysis, consistent with subsurface film growth [17]. Additional cycling eventually results in a thin film coalescence, after which ALD growth rates decrease to values close to what would be expected on an ALD thin film surface.

3.2. Polyvinyl alcohol

Polyvinyl alcohol (PVA) is a water soluble, semicrystalline, atactic polymer with good adhesive properties often cast into films or spun into fibers. It has glass transition temperature of ~85 °C and its melting point ranges from ~180 °C when less hydrolyzed to 230 °C when more fully hydrolyzed. Its density is ~1.2–1.3 g/cm^3. Peng et al. [25] and Spagnola et al. [16] explored ALD nucleation and growth on electrospun PVA nanofibers 200–300 nm in diameter, and on cast thin films, respectively. FTIR analysis was used [16] to examine the reactions between TMA and PVA at 90 °C, and results are shown in Fig. 4. The spectrum for the untreated PVA includes features expected for PVA as well as modes associated with acetate groups, indicating some material impurity. Specifically, features [45] include O—H stretch at 3380 cm^{-1} and CH_2 asymmetric stretch at 2910 cm^{-1}, and C═O stretch at 1736 cm^{-1}. Other modes include CH_2 scissors coupled with O—H deformation at 1433 cm^{-1}, CH_3 symmetric deformation at 1374 cm^{-1}, C—O (acetate) stretching at 1255 cm^{-1} and C—O (alcohol) stretching at 1096 cm^{-1}. After the first TMA exposure, negative-going features show a decrease in O—H and acetate C═O and C—O modes. Other modes appear at 1200 and 700 cm^{-1} corresponding to O—Al—CH_3 groups. Upon water exposure, the —OH modes increase and the Al—CH_3 features decrease in intensity. The ALD sequence leads to overall loss in CH_2

Table 1
Relative extent of TMA reaction with various polymers.

Polymer	Characteristic group	Relative extent of TMA reaction: # of "Al—CH$_3$ monolayers" from IR
Polyolefin (PP fiber)	C—C	<10
Polyvinyl Alcohol (PVA fiber)	C—OH	~24 ± 6
Polyamide (PA-6)	C—(C=O)—NH—C	$\sim 5.9 \pm 0.9 \times 10^2$
Polyester (PBT)		$\sim 1.8 \pm 0.3 \times 10^4$
Polyester (PET)	C—(C=O)—O—C	$\sim 8.3 \pm 0.6 \times 10^4$
Polyester (PLA)		$\sim 3.1 \pm 0.3 \times 10^3$
Polycarbonate (PC)	C—O—(C=O)—O—C	$\sim 9.1 \pm 1.8 \times 10^2$
Poly methyl methacrylate (PMMA)	C—(C=O)—O—C	$\sim 1.0 \pm 0.2 \times 10^3$
Polyethylene Oxide (PEO)	C—O—C	$\sim 6.5 \pm 0.6 \times 10^4$

Adapted from Ref. [24].

stretching, and affects the acetate modes at 1736 cm^{-1}. Repeating the TMA/H_2O cycle leads to the same characteristic spectrum changes but the magnitude of the change is smaller.

Gong and Parsons [24] quantified the infrared absorbance change after TMA exposure on PVA and other polymers, and the results are presented in Table 1. The change in IR absorbance indicates that TMA exposure leads to the equivalent of ~24 "Al—CH$_3$ monolayers" on the PVA. These reactive units are primarily within the polymer subsurface and will react during the next water step leading to multilayer growth. This film can then prevent the precursor from penetrating deep into the polymer bulk during the next TMA/water cycle, and film coalescence after a few cycles leads to normal ALD growth rates of ~1.1 Å/cycle. TEM analysis of Al_2O_3 growth rates on PVA fibers [25] shows a higher growth rate during the initial few ALD cycles, consistent with the IR analysis. Therefore, the TMA/water ALD process on PVA closely follows that for ALD on a solid surface, except during the first few cycles where some excess growth may proceed.

Other polymer materials show trends similar to that for ALD Al_2O_3 on PVA. A common example is during TMA/water ALD on cotton cellulose. In this case, surface energy analysis, IR transmission and TEM (shown for example in Fig. 1) indicate growth is limited to the surface or near-surface of cotton fibers. This results in unexpected trends in surface wetting, for example, for cotton fibers and fabrics exposed to ALD Al_2O_3 [32,33].

3.3. Polyamide-6

Polyamide-6, or nylon-6, is a semicrystalline polymer widely used for fibers, filaments and ropes for its mechanical strength, elasticity and luster. Its melting point is ~220 °C and T_g is ~50 °C. It readily absorbs water and its density ranges from ~1.1 to 1.2 g/cm^3. Infrared absorbance data collected during ALD Al_2O_3 at 80 °C on a thin polyamide-6 film is shown in Fig. 5(a), along with TEM images of ALD-coated fibers. The absorbance of an untreated nylon-6 film shows a hydrogen bonded N—H stretching mode at 3304 cm^{-1}, the C—H_2 asymmetric and symmetric stretching features at 2930 and 2860 cm^{-1} respectively, and the amide I (C=O stretch) feature at 1640 cm^{-1}. Also visible are the amide II (N—H bend/C—N stretch) and amide III (N—C=O skeletal vibration) bands at 1541 cm^{-1} and 1280 cm^{-1}, respectively [45]. Exposing the PA-6 film to TMA produces significant changes in the IR modes. Methyl rocking and deformation modes appear at 1437 cm^{-1}, 1190 cm^{-1} and 690 cm^{-1}, and the N—H feature at 3304 cm^{-1} and amide I feature at 1640 cm^{-1} decrease in intensity. A mode also appears at ~1580 cm^{-1}. Subsequent water exposure removed the Al—CH$_3$ features and produced

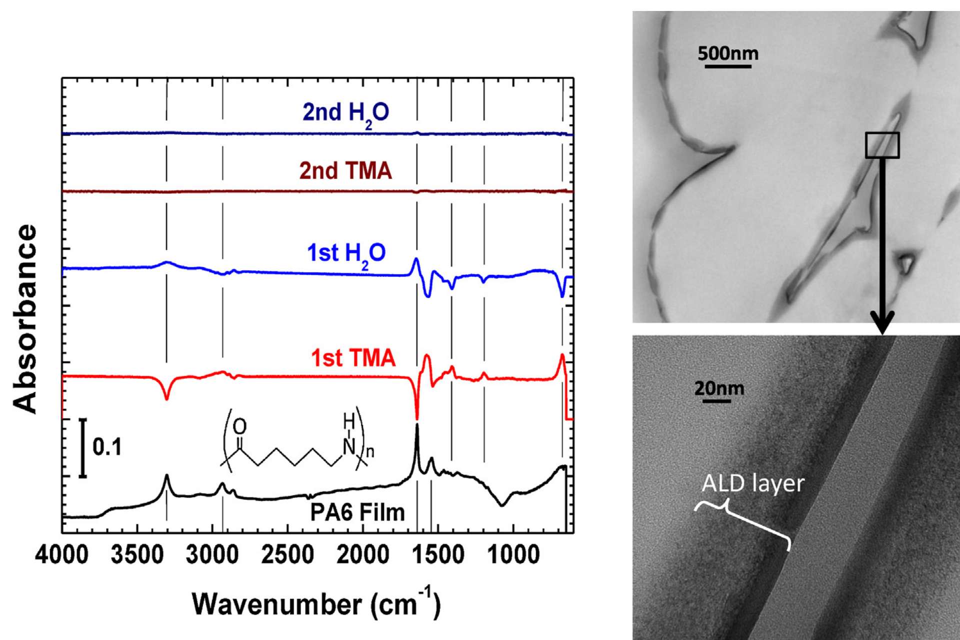

Fig. 5. Infrared and TEM results for TMA/water ALD on polyamide-6 at 80 °C. Substantial subsurface reaction is observed in both the IR and TEM data. A higher resolution TEM image shows a conformal and uniform film on the PA-6 fibers in addition to the subsurface reaction product layer.
Adapted from Ref. [26].

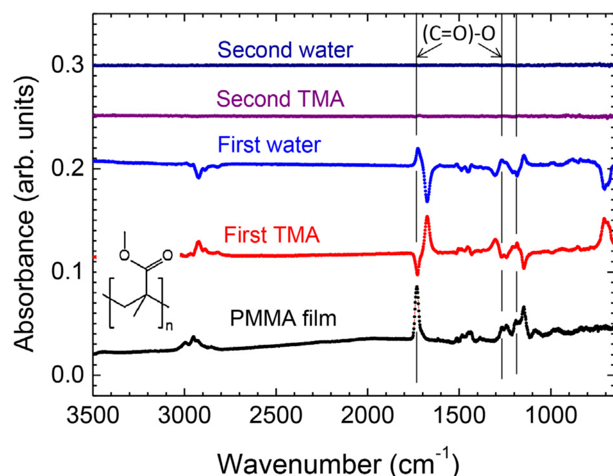

Fig. 6. Differential IR data during TMA/water ALD on poly(methyl methacrylate) at 80 °C. The data shows a strong interaction between the carbonyl and the TMA. The carbonyl stretch mode at ~1731 cm^{-1} decreases upon TMA exposure, then returns after water treatment.

Adapted from Ref. [24].

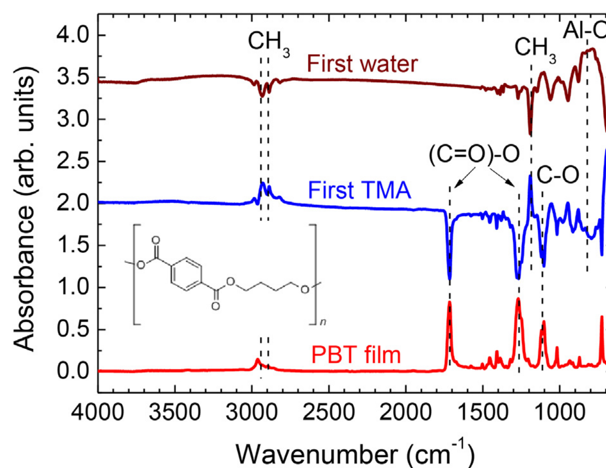

Fig. 7. IR data collected during TMA/water ALD on poly(butylene terephthalate) at 80 °C. Similar to the reaction on PMMA, the data shows a strong interaction between TMA and the carbonyl near ~1731 cm^{-1}. Unlike the PMMA, however, the carbonyl does not reappear after water exposure.

Adapted from Ref. [24].

an increase in Al—O stretching near ~700 cm^{-1}, consistent with water reaction with Al—CH_3 groups forming Al—OH. The mode at 1580 cm^{-1} disappears and the amide I carbonyl mode at 1640 cm^{-1} returns, with slightly less intensity. The TEM images in Fig. 5(b) show that the reactants diffuse a substantial distance beneath the polymer surface during ALD at 90 °C [16]. Recent work by Sun et al. further shows that the diffusion of TMA in PA-6 is strongly temperature dependent, with more diffusion at 60 °C and much less diffusion at 120 °C [20]. The IR data is consistent with TMA coordinating to the most Lewis basic site of the polymer, i.e. the oxygen of the amide moiety. In this scheme, the coordination leads to a proton transfer, methane evolution, and Al—O covalent bond formation. This is consistent with loss of hydrogen bonding as observed in the IR data. The amide moiety is then further degraded by the presence of the TMA. This is confirmed in the IR data due to the amide only partially reforming upon exposure to the water dose. After subsequent TMA/water cycles, the amide no longer reforms, and is presumed to be degraded completely.

3.4. Poly(methyl methacrylate)

Poly(methyl methacrylate) (PMMA) is a highly transparent thermoplastic polymer with $T_g \sim 100$ °C. Infrared spectra collected during TMA/water exposure on a ~200 nm thick PMMA film at 80 °C are shown in Fig. 6 [24]. The starting PMMA shows CH_2 asymmetric and symmetric stretching modes at 2930 and 2860 cm^{-1}, and the carbonyl C═O and ester C—O stretching features at 1731 cm^{-1} and 1260 cm^{-1}, respectively [45]. The TMA exposure leads to a decrease in C═O and C—O modes, and a new mode appears at 1675 cm^{-1}. The water exposure removes Al—CH_3 modes and produces the expected increase in Al—O mode at ~700 cm^{-1}. Water also causes the C—O ester feature to return at ~1260 cm^{-1}. In addition, the mode at 1675 cm^{-1} is removed and the carbonyl stretch returns to the spectrum, shifted slightly from 1731 to ~1725 cm^{-1}. The shift in the recreated C═O mode likely indicates polymer degradation. This could occur, for example, by formation of a ketone in place of the original ester group. The trend in carbonyl mode change is similar to that observed during TMA exposure to polyamide, as shown in Fig. 5(a), except after water exposure, the recreated C═O mode is at the same position as in the starting material because the original functional group is maintained.

3.5. Polyesters

Polyesters refer to the class of polymers containing an ester group in the polymer backbone. A common example is poly(ethylene terephthalate) (PET) which is used for many consumer products such as textile fibers and beverage bottles. It has a high melting point, ~250 °C, and its T_g is about 70–80 °C. A common related polyester is poly(butylene terephthalate) (PBT) used in electrical insulation, and it has a melting point near ~240 °C. In-situ FTIR spectra collected during TMA and water exposure on a PBT film at 80 °C are shown in Fig. 7. The spectrum for PBT includes modes for C═O stretch at ~1720 cm^{-1}, C—O stretch at ~1270 cm^{-1}, C—O—C stretch at ~1100 cm^{-1} and CH_2 symmetric and asymmetric stretch at ~2860 and 2925 cm^{-1}, respectively. After TMA exposure at 80 °C, negative-going modes indicate removal of carbonyl at ~1720 and 1260 cm^{-1}. New features at ~2960 cm^{-1} and 1200 cm^{-1} correspond to Al—CH_3 stretching and deformation modes. The new mode also appears at 680 cm^{-1} which is ascribed to Al—C bonds formed upon the TMA reaction. The magnitude of the absorbance change is consistent with very deep penetration and reaction of the TMA in the PBT polymer [24].

The infrared data shows reactions similar to those during TMA exposure on PMMA and PA-6, with one important difference. As noted above for PMMA and PA-6, the decrease in the carbonyl mode upon TMA exposure leads to a new peak at lower wavenumber, and after water exposure the low-wavenumber peak disappears, recreating the C═O stretch mode. For the PBT substrate, TMA exposure removes the carbonyl peak, but unlike the PMMA, no low-wavenumber feature appears. Moreover, the lost carbonyl in the PBT does not appear again after water exposure.

Infrared analysis of TMA exposure on other polymers containing carbonyl groups [24] shows TMA reaction with poly(ethylene terephthalate) and polycarbonate to be similar to PBT, i.e. the carbonyl group reacts with TMA without producing the low-wavenumber mode. The low-wavenumber mode does appear after TMA exposure to polylactic acid, but similar to PBT, the carbonyl does not return after water exposure to PET, PC and PLA. The difference between the carbonyl environments in these polymers and how the environment can affect reactivity is further revealed by analyzing the overall extent of reaction between the polymers and TMA.

3.6. Quantitative analysis

As mentioned above, Gong and Parsons [24] used FTIR spectra to quantitatively analyze the extent of TMA reaction at 80 °C with different polymers under a fixed set of process conditions, and results are presented in Table 1. For the analysis, polymer films several hundred nanometers thick were spun-cast onto high resistivity IR transparent silicon wafers then mounted in a homemade ALD reactor capable of in situ transmission infrared spectroscopy. The sample was aligned with its surface normal parallel to the IR beam path and perpendicular to the reactant gas flow. For each polymer film, the change in absorbance of various CH_3 modes was monitored after TMA exposure. The extent of reaction was then quantified by comparing the absorbance change to that observed after TMA saturation on anodic aluminum oxide, where the changes scaled linearly with the known AAO surface area in the beam path. The extent of reaction is expected to depend on temperature and exposure time, so the comparisons in Table 1 hold for the specific conditions used (60 s TMA at 80 °C).

The results in Table 1 show a relatively small extent of reaction on polyolefin and the polyvinyl alcohol substrates, and a larger extent of reaction on the other polymers studied. The extent of reaction is similar on PP and PVA even though the IR data in Figs. 3 and 4 show very different ALD nucleation mechanisms for these materials. The small extent of reaction on the PVA is consistent with relatively fast TMA nucleation on available reactive groups. On the other hand, the data in Fig. 3 shows that exposing polyolefin to TMA can change the IR modes substantially, but the under conditions used for the quantitative analysis, the change in CH_3 modes was relatively small. This is consistent with the TMA readily diffusing in and out of the polyolefin without a significant amount of reaction occurring with the polymer.

Most of the polymers listed in Table 1 all show a much larger extent of reaction upon TMA exposure, consistent with more extensive diffusion under the polymer surface. It is important to note that the extent of reaction is also expected to be influenced by the detailed nature of the reactive group in the polymer. The more reactive polymers in Table 1 all contain nucleophilic functional groups, such as C=O in the polyesters and polyamide and C—O—C in the polyethers. The PET and PMMA, for example, both contain —(C=O)—O— groups, but the carbonyl carbon is in the polymer backbone in PET, whereas it is in a side-chain in PMMA. The PET shows more than 10× larger extent of reaction with TMA that does the PMMA. The difference in the local environment around the carbonyl group is important to understand the distinct reactions that occur. Further discussion regarding mechanisms for this and other observations are presented in the following section.

4. Discussion

Polypropylene is an example of an inert polymer that can be coated uniformly by ALD. Results show that during ALD using TMA and water, the TMA diffuses into the near surface region of the polymer where it is kinetically trapped. The TMA will then react with water during the second half-cycle step to form nuclei beneath or at the polymer surface. The extent of reactant diffusion and the depth of the sub-surface growth depend on the substrate temperature, and they are also expected to be affected by exposure time. The extent of sub-surface growth strongly affects the resulting surface roughness as well as the structure of the polymer/film interface.

On polymers such as PVA or cellulose where there is a large density of reactive groups, the ALD reaction can be limited to the top surface of the polymer. The large number of available reaction sites can lead to film growth that is faster during the first few ALD cycles than during later "steady-state" ALD. Fast initial growth could be due to excess water, bound at or near the surface in hydrogen bonded states or more tightly held in surface creases, crevices or small structures. The high density of surface functional groups lets a cohesive film coating form quickly, leading to regular ALD after the first few cycles.

Other polymers with different reactive groups show very different reaction trends. The carbonyl site is the most Lewis basic functionality in the polyamides or polyesters, so it is expected to coordinate with the TMA Lewis acid to form an aluminum-oxygen-alkyl unit. The polyamide-6 has reactive carbonyl and amine groups which provide strong hydrogen bonding between neighboring chains. The IR data shows the TMA exposure influences both groups. The coupling between TMA and carbonyl or amine will affect the strong hydrogen bond interaction between them [16]. Disruption of the hydrogen bonding could act to "open up" the polymer chain network, promoting further TMA diffusion into the subsurface region. This is expected to affect the mechanical properties of the polymer.

In the polyamide and polyester substrates, the data is consistent with TMA first coordinating to the carbonyl moiety. A reaction forming a covalent aluminum–oxygen bond can proceed either via resonance modes (for the polyamide) or methyl migration from TMA to the electrophilic carbon site of the carbonyl moiety (for the PMMA or polyester). A schematic diagram for a possible reaction mechanism for TMA/water reaction with PMMA is shown in Fig. 8. In this scenario, the carbonyl stretch is eliminated by the TMA reaction with the carbonyl forming a side-chain acetal group. The subsequent water dose reforms the carbonyl but it is in the form of a ketone instead of the starting ester. The carbonyl is available for further reaction with TMA (not shown).

The starting location of the reactive functional group (amide/ester/alcohol) on the backbone or side-chain plays a role in determining the end reaction product. The carbonyl in the polymer backbone can provide reaction routes that lead to polymer chain dissociation, forming products that do not contain the carbonyl. Hence, these reactions do not show carbonyl modes returning in the IR spectra after the water exposure. A different configuration for the carbonyl group, e.g. when it is bound as a side-chain moiety, can open reaction pathways that reform the carbonyl after water exposure, as shown for example for TMA/water on PMMA in Fig. 8. The carbonyl in the side chain in this case is more likely to react without significantly impacting the backbone stability. In addition, more sterically accessible reactive sites can increase the rate of TMA coordination. This could, in turn, allow TMA to be released from the adduct and diffuse to bind at another site. Significant diffusion will occur if the barrier to the final product state is larger than the barrier to diffusion.

Another important aspect to consider is the catalytic effect of the TMA. Organo-aluminum compounds bound to an electron pair donor state are known to accelerate reactions in adjacent bonds [41]. Therefore, a TMA molecule in the adduct state can activate a neighboring ester or amide functional groups for nucleophilic attack and/or nucleophilic migration.

Recent studies of TiO_2 ALD onto PA-6 show that different titanium precursors will produce very different results. Specifically, $TiCl_4$ was observed to diffuse and react subsurface, whereas titanium isopropoxide reacted on the surface producing an abrupt organic/inorganic interface [46]. Like TMA, $TiCl_4$ is also a strong Lewis acid, so it my diffuse into the polymer and react with PA-6 through similar Lewis acid/base adducts. In addition, the larger size and the steric effects of the isopropoxide ligands may limit the titanium isopropoxide reactivity and ability to diffuse within the polymer. The ability to control the reaction between ALD precursors and polymers opens new opportunities in ALD materials processing. For example, using polymer materials with multiple components on the micro-, nano- or macro-scale, ALD precursors can be chosen to selectively react with different parts of the structure [8,39,47,48]. The ALD reactants can also diffuse throughout

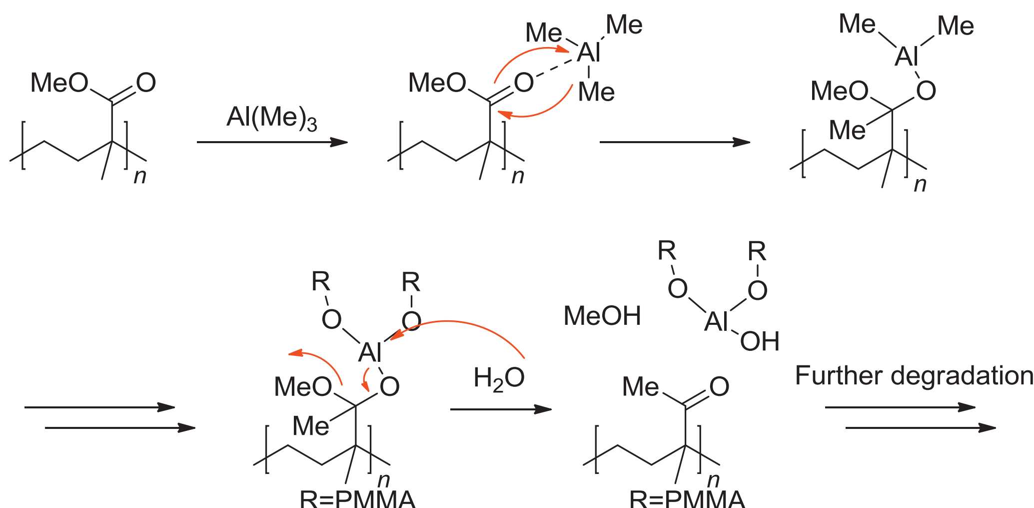

Fig. 8. Possible mechanism scheme for Lewis-acidic TMA reaction with the Lewis-basic carbonyl group in PMMA, followed by reaction with water. The TMA forms an adduct with the carbonyl, followed by methyl transfer to the carbon to form an acetal unit. The reaction can also occur with neighboring polymer chains to form Al—(OR—)$_3$ centers. Reaction with water then reforms the carbonyl in a ketone unit rather than the starting ester, as evidenced by the shifted IR mode. The product is then available to react with TMA. Remaining —R—O—Al—OH sites can also react with TMA to nucleate aluminum oxide ALD sites.

the polymer bulk, to saturate the functional groups present in the polymer chain. Upon further reaction, this can effectively transform the polymer into a new organic/inorganic material where the initial shape is defined by the starting polymer but the material properties are defined by the ALD precursor and reaction sequence. The chemical mechanisms associated with ALD on polymers are strongly influenced by the nature of the polymer and ALD precursor, and the broad knowledge and understanding of ALD nucleation on hard surfaces does not translate readily to ALD on soft materials and interfaces.

5. Summary

Solutions to a growing number of problems involving ALD reactions with organic polymers will require a more full and basic understanding of the chemical mechanisms associated with precursor and reactant species interactions with organic functional groups and polymer chains. Significant work has begun to show the applications, capabilities and limits for ALD on polymers. This article summarizes results demonstrating that reaction processes during TMA/H_2O on polymer materials depend strongly on the starting polymer. The large difference in reactions on various polymers suggests that ALD will also depend on the precursor being used as well as the detailed process conditions. Clean surface growth under one set of conditions (for example, ALD Al_2O_3 on polypropylene at low temperature) can transition to substantial sub-surface diffusion and reaction for the same polymer and coating material under somewhat different conditions (e.g. higher deposition temperature). We also highlight the important point that reactive intermediates that form at moderate temperatures when metal-containing precursors interact with polymer functional groups may be important in defining the overall ALD reaction product. When precursors diffuse sub-surface and react with available polymer functional groups, the reaction can become bulk saturated, similar to surface saturation in an ALD half-reaction. This leads to new possibilities for materials formation using a binary sequence of self-limiting reactions, well beyond planar thin film deposition.

Acknowledgement

Support is acknowledged from the US National Science Foundation under Grant # 1034374.

References

[1] M. Benmalek, H.M. Dunlop, Surf. Coat. Technol. 76 (1995) 821.
[2] K.L. Tan, L.L. Woon, H.K. Wong, E.T. Kang, K.G. Neoh, Macromolecules 26 (1993) 2832.
[3] C. Bichler, T. Kerbstadt, H.C. Langowski, U. Moosheimer, Surf. Coat. Technol. 112 (1999) 373.
[4] T. Yuranova, A.G. Rincon, A. Bozzi, S. Parra, C. Pulgarin, P. Albers, J. Kiwi, J. Photochem. Photobiol. A: Chem. 161 (2003) 27–34.
[5] T. Hirvikorpi, M. Vähä-Nissi, A. Harlin, M. Karppinen, Thin Solid Films 518 (2010) 5463–5466.
[6] G.N. Parsons, S.M. George, M. Knez, MRS Bull. 36 (2011) 865–871.
[7] G.N. Parsons, in: N. Pinna, M. Knez (Eds.), Atomic Layer Deposition of Nanostructured Materials, Wiley-VCH/Verlag GmbH & Co. KGaA, 2012.
[8] M. Knez, Semicond. Sci. Technol. 27 (2012) 074001.
[9] M.D. Groner, S.M. George, R.S. McLean, P.F. Carcia, Appl. Phys. Lett. 88 (2006) 051907.
[10] R. Cooper, H.P. Upadhyaya, T.K. Minton, M.R. Berman, X. Du, S.M. George, Thin Solid Films 516 (2008) 4036–4039.
[11] F.H. Fabreguette, S.M. George, Thin Solid Films 515 (2007) 7177–7180.
[12] A.W. Ott, R.P.H. Chang, Mater. Chem. Phys. 58 (1999) 132–138.
[13] J.D. Ferguson, A.W. Weimer, S.M. George, Chem. Mater. 16 (2004) 5602–5609.
[14] C.A. Wilson, R.K. Grubbs, S.M. George, Chem. Mater. 17 (2005) 5625–5634.
[15] M. Puttaswamy, K.B. Haugshøj, L. Højslet Christensen, P. Kingshott, Chem. Eur. J. 16 (2010) 13925–13929.
[16] J.C. Spagnola, B. Gong, S.A. Arvidson, J.S. Jur, S.A. Khan, G.N. Parsons, J. Mater. Chem. 20 (2010) 4213.
[17] J.S. Jur, J.C. Spagnola, K. Lee, B. Gong, Q. Peng, G.N. Parsons, Langmuir 26 (2010) 8239–8244.
[18] M. Vähä-Nissi, E. Kauppi, K. Sahagian, L.-S. Johansson, M.S. Peresin, J. Sievänen, A. Harlin, Thin Solid Films 522 (2012) 50–57.
[19] C.J. Oldham, B. Gong, J.C. Spagnola, J.S. Jur, K.J. Senecal, T.A. Godfrey, G.N. Parsons, J. Electrochem. Soc. 158 (2011) D549.
[20] Y. Sun, P. Padbury, H.I. Akyildiz, M.P. Goertz, J.A. Palmer, J.S. Jur, Chem. Vapor Deposit. 19 (4–6) (2013) 134–141, http://dx.doi.org/10.1002/cvde.201207042.
[21] M. Kemell, E. Färm, M. Ritala, M. Leskelä, Eur. Polym. J. 44 (2008) 3564–3570.
[22] A. Sinha, D.W. Hess, C.L. Henderson, J. Vac. Sci. Technol. B 25 (2007) (1721).
[23] T.O. Kääriäinen, D.C. Cameron, M. Tanttari, Plasma Processes Polym. 6 (2009) 631–641.
[24] B. Gong, G.N. Parsons, J. Mater. Chem. 22 (2012) 15672.
[25] Q. Peng, X.-Y. Sun, J.C. Spagnola, G.K. Hyde, R.J. Spontak, G.N. Parsons, Nano Lett. 7 (2007) 719–722.
[26] J.C. Spagnola, B. Gong, G.N. Parsons, J. Vac. Sci. Technol. A 28 (2010) 1330.
[27] B. Gong, J.C. Spagnola, G.N. Parsons, J. Vac. Sci. Technol. A 30 (2012) 01A156.
[28] K.J. Hughes, J.R. Engstrom, J. Vac. Sci. Technol. A 30 (2012) 01A102.
[29] S.-H.K. Park, J. Oh, C.-S. Hwang, J.-I. Lee, Y.S. Yang, H.Y. Chu, Electrochem. Solid-State Lett. 8 (2005) H21.
[30] M. Kemell, V. Pore, M. Ritala, M. Leskelä, Chem. Vapor Deposit. 12 (2006) 419.
[31] G.K. Hyde, K.J. Park, S.M. Stewart, J.P. Hinestroza, G.N. Parsons, Langmuir 23 (2007) 9844.
[32] G.K. Hyde, G. Scarel, J.C. Spagnola, Q. Peng, K. Lee, B. Gong, K.G. Roberts, K.M. Roth, C.A. Hanson, C.K. Devine, S.M. Stewart, D. Hojo, J.-S. Na, J.S. Jur, G.N. Parsons, Langmuir 26 (2010) 2550.
[33] K. Lee, J.S. Jur, D.H. Kim, G.N. Parsons, J. Vac. Sci. Technol. A 30 (2012) 01A163.

[34] M. Kemell, V. Pore, M. Ritala, M. Leskelä, M. Lindén, J. Am. Chem. Soc. 127 (2005) 14178.
[35] S.-M. Lee, E. Pippel, U. Gosele, C. Dresbach, Y. Qin, C.V. Chandran, T. Brauniger, G. Hause, M. Knez, Science 324 (2009) 488.
[36] B. Gong, Q. Peng, J.S. Jur, C.K. Devine, K. Lee, G.N. Parsons, Chem. Mater. 23 (2011) 3476.
[37] H. Shin, D.K. Jeong, J. Lee, M.M. Sung, J. Kim, Adv. Mater. 16 (2004) 1197.
[38] J.S. King, E. Graugnard, O.M. Roche, D.N. Sharp, J. Scrimgeour, R.G. Denning, A.J. Turberfield, C.J. Summers, Adv. Mater. 18 (2006) 1561.
[39] Q. Peng, Y.-C. Tseng, S.B. Darling, J.W. Elam, Adv. Mater. 22 (2010) 5129.
[40] Y. Xu, C.B. Musgrave, Chem. Mater. 16 (2004) 646.
[41] T. Suzuki, H. Saimoto, H. Tomioka, K. Oshima, H. Nozaki, Tetrahedron Lett. 23 (1982) 3597.
[42] A. Dube, M. Sharma, P.F. Ma, J.R. Engstrom, Appl. Phys. Lett. 89 (2006) 164108.
[43] N.P. Kobayashi, R.S. Williams, Chem. Mater. 20 (2008) 5356.
[44] M. Li, M. Dai, Y.J. Chabal, Langmuir 25 (2009) (1911).
[45] I. Noda, A.E. Dowrey, J.L. Haynes, C. Marcott, in: J.E. Mark (Ed.), Physical Properties of Polymers Handbook, Springer, New York, 2007.
[46] C.K. Devine, C.J. Oldham, Howard, J. Walls, G.N. Parsons, J. Vac. Sci. Technol. (2013), in press.
[47] Y. Wang, Y. Qin, A. Berger, E. Yau, C. He, L. Zhang, U. Gösele, M. Knez, M. Steinhart, Adv. Mater. 21 (2009) 2763.
[48] B. Gong, J.C. Spagnola, S.A. Arvidson, S.A. Khan, G.N. Parsons, Polymer 53 (2012) 463.